ACS APPLIED MATERIALS & INTERFACES

www.acsami.org

Research Article

Reactive Extrusion of Nonmigratory Active and Intelligent Packaging

Halle N. Redfearn, Matthew K. Warren, and Julie M. Goddard*

Cite This: *ACS Appl. Mater. Interfaces* 2023, 15, 29511−29524

Read Online

ACCESS | Metrics & More | Article Recommendations | Supporting Information

ABSTRACT: The environmental and economic burden of food waste demands new preservation technologies to reduce the degradative actions of spoilage such as moisture, oxygen, and microorganisms. Direct food additives can help maintain product quality; however, the limited life span of these additives combined with consumer desire for "clean label" products has motivated research into new food manufacturing technologies like active and intelligent packaging that can prevent and detect food spoilage. In this work, curcumin was grafted to polypropylene (PP-*g*-Cur) via reactive extrusion to produce nonmigratory active and intelligent packaging through a solvent-free, efficient, and continuous method. Immobilization of curcumin was confirmed by a standard migration assay exhibiting a maximum of 0.011 mg/cm^2 migration, significantly below the EU migratory limit for food contact materials (0.1 mg/cm^2). Compared to native PP films, PP-*g*-Cur films blocked 93% of UV light while retaining 64% transparency in the visible region, allowing for desirable product visibility while inhibiting UV degradation of packaged goods. While the ability of PP-*g*-Cur to inhibit growth of *E. coli* and *L. monocytogenes* was insignificant compared to control PP, free curcumin exhibited poor bacterial inhibition as well, suggesting that without hydrophilic modification, native curcumin has limited antimicrobial efficacy. PP-*g*-Cur films displayed significant radical scavenging in both organic (11.71 ± 3.02 $\text{Trolox}_{\text{Eq}}$ (nmol/cm^2)) and aqueous (3.18 ± 1.04 $\text{Trolox}_{\text{Eq}}$ (nmol/cm^2)) matrices, exhibiting potential for antioxidant behavior in both lipophilic and hydrophilic applications. Finally, when PP-*g*-Cur films were exposed to ammonia, an indicator of microbial growth, the color visually and quantitatively changed from yellow to red, demonstrating potential to indicate spoilage. These findings demonstrate the potential of a scalable technology to produce active and intelligent packaging to limit food waste and advance the capabilities of functional materials in a variety of applications.

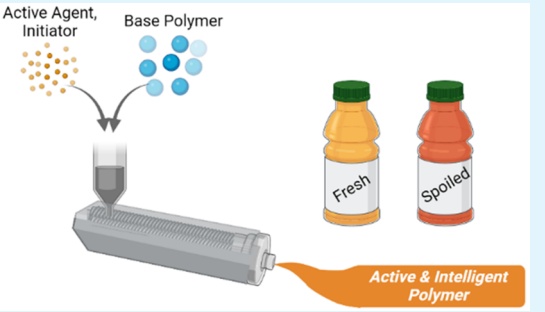

KEYWORDS: *active packaging, reactive extrusion, nonmigratory, functional polymer, curcumin*

INTRODUCTION

The USDA estimates that 30−40% of the total food supply in the United States goes to waste each year, with approximately 31% of that waste occurring at the consumer and retail levels.[1] Microbial growth and oxidation are the two prominent driving forces of food spoilage due to degradative mechanisms that alter the sensory characteristics of products and lead to consumer rejection.[2] While unit operations such as ultrahigh temperature processing (UHT) and product formulation techniques such as acidification are used to inhibit microbial growth,[3] survival of heat-resistant microorganisms[4] as well as post-process contamination[5] has prompted the use of antimicrobial preservatives to prevent microbial spoilage. Similarly, methods to mitigate oxidative degradation such as vacuum sealing, gas flushing, and high-barrier packaging materials are imperfect,[6] necessitating the use of antioxidant preservatives in products susceptible to oxidative degradation. Traditional preservatives rely on the direct addition of active compounds to the food matrix, but consumer trends toward "clean" labels and increasing demand for longer shelf life have prompted research in new preservation technologies.[7] Active packaging materials such as those incorporating polyphenol antimicrobial and antioxidant agents[8] have the potential to prolong preservative functionality through controlled release of active compounds and ease consumer label concerns through use of natural preservatives. However, migratory active packaging has several drawbacks, including the necessary approval of active agents as direct additives, adverse impact to material mechanical properties, and often negative effects on product quality.[9,10] Thus, there has been a new wave of active packaging technologies in which the active ligand is covalently bound to the packaging matrix to render it immobilized/nonmigratory. Prior research has demonstrated that covalent

Received: May 15, 2023
Accepted: May 25, 2023
Published: June 9, 2023

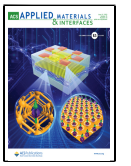

https://doi.org/10.1021/acsami.3c06589
ACS Appl. Mater. Interfaces 2023, 15, 29511−29524

modification of polypropylene (PP) with iminodiacetic acid,[11] acrylic acid,[12] tannic acid,[13] and polylysine[14] can extend the shelf life of food without the active agent leaching into the product. Compared to migratory active packaging and direct additives, nonmigratory active packaging can enhance the mechanical and optical properties of the packaging, prolong the life span of the active packaging functionality, and limit the effects of preservatives on the quality—flavor, texture, and color—of the food.[10]

While active packaging technology and research has progressed at a rapid pace, commercial adoption has been limited by manufacturing process scale-up and regulatory requirements to ensure safety.[15] Reactive extrusion provides an alternative to traditional thermoplastic polymer processing methods (solution casting, compression molding, etc.) with the potential to reduce time, labor, cost, and complexity of manufacturing. Previous work in the development of functional polymers has demonstrated the promise of reactive extrusion as a solvent-free, efficient, continuous, and single-step process[16] for the covalent attachment of active compounds to thermoplastic polymers. For instance, *N*-halamine was radically grafted to PP for biocidal medical devices,[17] poly(lactic acid) (PLA) was covalently modified with poly(ethylene glycol) to improve mechanical properties,[18] and poly(vinyl alcohol-*co*-ethylene) was functionalized with 2,4-diamino-6-diallylamino-1,3,5-triazine (NDAM) for antimicrobial medical and other hygienic products.[19] In recent years, our group has employed reactive extrusion for the synthesis of nonmigratory active packaging. Herskovitz et al. demonstrated the antioxidant capacity of PLA grafted with nitrilotriacetic acid by reactive extrusion,[20,21] and Doshna et al. reported the antimicrobial efficacy of polylysine radically grafted to PP by reactive extrusion.[14] Without the need for downstream processing, large volumes of solvent, or specialized equipment necessary for wet chemical or bench scale grafting methods, reactive extrusion provides an economic and potentially greener method to produce active materials.

Curcumin is an antioxidant and antimicrobial natural polyphenol responsible for the orange-yellow color and therapeutic value of *Curcumin longa* (turmeric). As a biologically active GRAS (generally recognized as safe) compound, curcumin has a long history of use in medicine, food coloring and flavoring, and preservation.[22] The antimicrobial properties of curcumin are derived from the inhibitory effect on bacterial cell proliferation and disruption of membrane proteins in fungi.[23] The antioxidant capacity of curcumin is attributed to its radical scavenging capacity by both hydrogen and electron donation and metal chelating capacity by formation of complexes with the diketone.[24] Curcumin also has the ability to change color in alkaline conditions, such as those produced by meat and seafood during spoilage.[25] Thus, curcumin is an ideal candidate for active and intelligent packaging applications, in which it has the potential to integrate antimicrobial and antioxidant function to mitigate product spoilage and color indicating features to visually signify product spoilage. Accordingly, there has been significant work in the development of active packaging materials blended with curcumin with preserved functional performance, including low-density polyethylene (LDPE),[26] poly(lactic acid) (PLA),[27] and poly(butylene adipate terephthalate) (PBAT).[28] Previous research has also demonstrated the intelligent properties of materials blended with curcumin to indicate spoilage of beef and silver carp,[26] shrimp,[29] and chicken breast.[30] While these technologies demonstrate the retained functionality of curcumin embedded in hydrophobic polymer matrices, to the best of the authors' knowledge there has been no reports of covalent immobilization of curcumin to develop nonmigratory packaging capable of both intelligent and preservative action.

The aim of this study was to functionalize a thermoplastic polymer common in food packaging, polypropylene (PP), with curcumin through an industrially translatable method to produce active and intelligent packaging. The functionalization was accomplished through radical grafting with a peroxide initiator via reactive extrusion. Previous research demonstrated radical grafting of gallic acid onto chitosan using wet chemical methods, which suggested the radical initially forms on the phenolic oxygen of the polyphenol by hydrogen abstraction.[31−34] Thus, curcumin can be grafted by the phenoxy radical, or it can undergo an intermolecular radical transfer process resulting in radical grafting of the aromatic ring at the ortho or para position relative to the hydroxyl.[31,35,36] Previous works have also demonstrated the ability of curcumin to undergo hydrogen abstraction to form a carbon-centered radical at the β-diketone moiety, which would also undergo an intermolecular radical transfer reaction, resulting in grafting by the enolic alkoxy radical.[37] Thus, curcumin is capable of radical grafting via multiple pathways due to its various radical scavenging mechanisms. While these previous works demonstrated covalent immobilization of polyphenols via radical grafting with retained antioxidant activity, they utilize lengthy (over 24 h) and multistep processes that limit pragmatic commercial translation. Radical grafting of curcumin onto polypropylene via reactive extrusion has great potential to produce nonmigratory active packaging through a scalable, environmentally friendlier, and economic method. To the authors' knowledge, this is the first time reactive extrusion has been used to produce nonmigratory multifunctional packaging, thus advancing the capabilities and commercial viability of functional materials both in food applications and beyond.

EXPERIMENTAL SECTION

Materials. L-Ascorbic acid, curcumin (cat. no. 8.20354, CAS no. 458-37-7), 2,2-diphenyl-1-picrylhydrazyl (DPPH), ethylenediaminetetraacetic acid calcium disodium salt (EDTA), glacial acetic acid, hydrochloric acid (trace-metal grade), (±)-6-hydroxy-2,5,7,8-tetramethylchromane-2-carboxylic acid (Trolox, 97%), imidazole (99%), polypropylene-*graft*-maleic anhydride (PP-*g*-MA) pellets (maleic anhydride 8−10 wt %, cat. no. 427845, CAS no. 25722-45-6), potassium persulfate (≥99%), sodium acetate trihydrate, sodium phosphate dibasic heptahydrate, and sodium phosphate monobasic monohydrate were purchased from MilliporeSigma (Burlington, MA). 2,2′-Azino-bis(3-ethylbenzothiazoline-6-sulfonic acid) diammonium salt (ABTS, 98%) and sodium hydroxide were purchased from Fisher Scientific (Fair Lawn, NJ). Dicumyl peroxide (DCP) was purchased from Krackeler Scientific (Albany, NY) and ground into a fine powder using a mortar and pestle. Ethanol (200 proof) was procured from Decon Laboratories (King of Prussia, PA). Polypropylene (PP) pellets (isotactic, cat. no. 130, CAS no. 9003-07-0) were obtained from Scientific Polymer (Ontario, NY). Grades U, E, and EX purge for the extruder were generously provided by Asahi Kasei Asaclean Americas (Parsippany, NJ). All reagents were used as received without further purification.

Synthesis and Characterization of Antioxidant Polypropylene (PP-*g*-Cur). *Preparation of Granulated Polypropylene and Polypropylene-graft-Maleic Anhydride Blend.* To facilitate homogenization of polymer pellets and reagent powders, isotactic PP and PP-*g*-MA were blended as described previously.[38] Briefly, PP was mechanically mixed with 50% w/w PP-*g*-MA and fed into a Process

https://doi.org/10.1021/acsami.3c06589
ACS Appl. Mater. Interfaces 2023, 15, 29511−29524

11 parallel twin screw extruder (Thermo Fisher Scientific, Waltham, MA) through an attached volumetric feeder (11 mm volumetric single screw feeder for process 11 [MK2] by Thermo Electron, Germany) at 7% the maximum rate. Isotactic PP without blending was also prepared as a control for all analyses. The pellets were processed at 250 rpm through a 1.5 mm die using the following temperature profile: Zone 2: 140 °C; Zone 3: 180 °C; Zone 4: 180 °C; Zone 5: 180 °C; Zone 6: 180 °C; Zone 7: 180 °C; Zone 8: 180 °C; and 190 °C at the die. The extruded polymer filament was fed into a Vericut Pelletizer (ThermoFisher Scientific, Waltham, ME) using the L1 setting to form 0.5 mm granules of blended PP and PP-*g*-MA. Granules were stored over anhydrous calcium sulfate desiccant for at least 24 h prior to further processing. To obtain polymer films, 1.5 g of polymer granules was placed in a single layer between two 5 mil Kapton films (Cole-Parmer, Vernon Hills, IL) and allowed to melt in a Fortin CRC Prepreg Mini Test Press at 180 °C for 2 min. Films were then pressed for 30 s to a thickness of 0.22 ± 0.04 mm and stored under calcium sulfate desiccant for at least 24 h. Films were immersed in absolute ethanol and shaken at 150 rpm for 2 h to wash any contaminants and ungrafted curcumin. Films were dried with filtered compressed air and stored over anhydrous calcium sulfate desiccant until further analysis. From this point forward, 50:50 w/w blended PP-*g*-MA: PP films and pellets will be termed simply PP-*g*-MA. Pure PP extruded, pelletized, pressed, and washed from this process will be termed PP and was used as the control for all experiments (Table 1).

Table 1. Concentrations (weight percent) of PP-*g*-MA, DCP, and Curcumin in Final Films[a]

sample ID	PP-*g*-MA% (w/w)	DCP% (w/w)	curcumin % (w/w)
PP	0	0	0
PP-*g*-MA/PP	25	0	0
PP-*g*-Cur1	0	0.5	1
PP-*g*-Cur2	0	0.5	2
PP/Cur1	0	0	1
PP/Cur2	0	0	2
PP-*g*-MA/PP-*g*-Cur1	25	0.25	0.5
PP-*g*-MA/PP-*g*-Cur2	25	0.25	1
PP-*g*-MA/PP/Cur1	25	0	0.5
PP-*g*-MA/PP/Cur2	25	0	1

[a]Remaining weight percent is composed of extruded and pelletized PP.

Preparation of Antioxidant Functionalized Polypropylene (PP-g-Cur) via Reactive Extrusion. Granulated PP (described above), dicumyl peroxide (DCP), and curcumin were used to synthesize antioxidant PP-*g*-Cur via radical grafting in the melt by reactive extrusion (Scheme 1, created with ChemDraw 20.1 by PerkinElmer, USA). DCP was received as large pellets, which were homogenized into a fine powder using a mortar and pestle and stored at 4 °C until further use. Granulated PP was mechanically mixed with 0.5% w/w powdered DCP and either 1% or 2% w/w curcumin and fed into a Process 11 parallel twin screw extruder (Thermo Fisher Scientific) through an attached volumetric feeder (11 mm volumetric single screw feeder for process 11 [MK2] by Thermo Electron, Germany) at 18% the maximum rate. Mixtures containing 1% and 2% w/w curcumin and granulated PP without DCP were also extruded as controls for the radical grafting reaction. The mixtures were processed at 150 rpm through a 1.5 mm die using the following temperature profile: Zone 2: 145 °C; Zone 3: 160 °C; Zone 4: 165 °C; Zone 5: 170 °C; Zone 6: 175 °C; Zone 7: 175 °C; Zone 8: 175 °C; and 185 °C at the die. It is important to note the mixing elements of the extruder were placed in Zones 3, 4, and 6, with the rest of the zones containing conveying elements. Extruded samples were pelletized, pressed, washed, and stored as described for granulated PP and PP-*g*-MA. Nomenclature for these samples is as follows: PP-*g*-Cur*X* for samples processed with DCP and PP/Cur*X* for samples processed without DCP, in which *X* refers to the weight percentage of curcumin and slashes indicate unreacted (melt blended without radical grafting) blends (Table 1).

Preparation of PP-g-Cur and PP-g-MA Blends. PP-*g*-MA was used as a compatibilizer to improve the optical and interfacial properties of PP-*g*-Cur. Granulated PP-*g*-MA was mechanically mixed with 50% w/w PP-*g*-Cur*X* or PP/Cur*X* (as a control for the radical grafting reaction) and extruded under the conditions described above for PP-*g*-Cur. To determine the impact of maleic anhydride (MA) on functional and physical properties, blends containing 50% w/w granulated PP with 50% w/w granulated PP-*g*-MA were also extruded under the same conditions. All extruded samples were pelletized, pressed, washed, and stored as described for granulated PP and PP-*g*-MA. Nomenclature for these blended samples is as follows: PP-*g*-MA/PP, PP-*g*-MA/PP-*g*-CurX, and PP-*g*-MA/PP/Cur*X*, where *X* refers to the weight percentage of curcumin and slashes indicate unreacted blends. The final compositions of all samples are listed (Table 1).

Film Thickness Measurements. The thicknesses of all films were measured using a Snapthick (iGaging , San Clemente, CA) 3-Way Digital Electronic Thickness Gauge accuracy of 0.02 mm. Measurements were taken on a single random location on each of three independent films from each of two independent batches per sample.

Characterizing the Interfacial, Chemistry, Thermal, and Optical Properties of PP-g-Cur Attenuated Total Reflectance Fourier Transform Infrared Spectroscopy (ATR-FTIR). ATR-FTIR using an IRPrestige FTIR spectrometer equipped with a diamond ATR crystal (Shimadzu Scientific Instruments Inc., Kyoto, Japan) was used to identify characteristic functional groups of each sample. Spectra were taken from the average of 32 scans using Happ−Genzel apodization and 4 cm^{-1} resolution with air as the background spectrum. Spectra of samples containing curcumin were compared against PP and PP-*g*-MA/PP negative controls. Origin Pro 2021b was used to baseline correct and graph all spectra. FTIR analysis was performed on two independent spots on each of two independent coupons for each of two independently prepared batches per sample. A random number generator was used to pick one of the eight collected spectra for each sample for reporting here.

Surface Dynamic Water Contact Angle Analysis. The advancing contact angle, receding contact angle, and hysteresis values for treated and control films were analyzed using an Attention Theta optical tensiometer (Biolin Scientific, Stockholm, Sweden) based on methods previously reported[20] with minor adjustments. Briefly, the advancing contact angle (θ_A) analysis was performed by depositing a deionized water droplet of ∼4 μL on the surface of each film. The syringe was inserted into the center of the droplet, and the size of the droplet was increased at a rate of 0.5 μL/s with images being recorded at 14 frames/s. The contact angle was analyzed using the Young−Laplace method, and the advancing contact angle was defined as the maximum stabilized mean contact angle prior to droplet's baseline advancing. Similarly, the receding contact angle (θ_R) was measured by reinserting the needle into the expanded droplet from the advancing contact angle procedure and decreasing the size of the droplet at a rate of 0.5 μL/s. The contact angle was recorded and analyzed using the same parameters as advancing but with the receding contact angle defined as the maximum stabilized mean contact angle prior to the droplet's baseline receding. Contact angle hysteresis was calculated as the difference between advancing and receding contact angle for each measurement. All measurements were performed on two different spots of two different coupons from two independently extruded batches of each sample (totaling eight measurements per treatment).

Thermal Analysis. Thermogravimetric analysis (TGA 5500, TA Instruments, New Castle, DE) was used to measure the thermal stability of polymers and curcumin powder (Figure S2). All samples were placed in a platinum pan and heated to 600 °C at a rate of 10 °C/min under nitrogen. Modulated differential scanning calorimetry (DSC 2500, TA Instruments, New Castle, DE) was used to determine the thermal properties of control and treated samples as well as curcumin powder (Figure S3). A heat−cool−heat method was used on samples sealed in aluminum pans, with an empty aluminum pan

https://doi.org/10.1021/acsami.3c06589
ACS Appl. Mater. Interfaces 2023, 15, 29511−29524

Scheme 1. Proposed Reaction Scheme for the Radical Grafting of Curcumin to PP during Reactive Extrusion to Form Polypropylene-*graft*-Curcumin (PP-*g*-Cur)

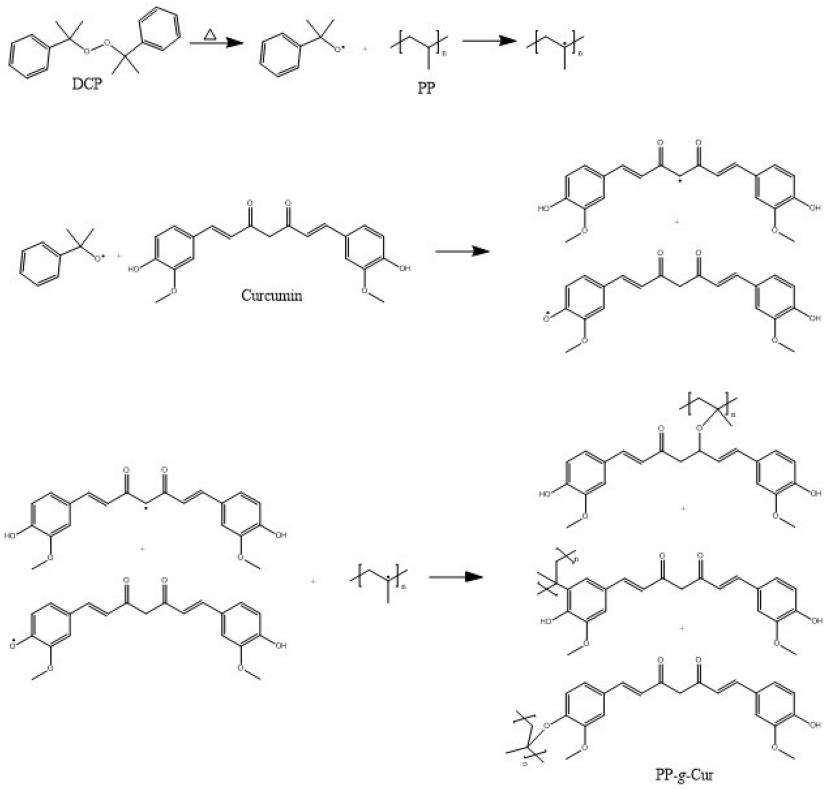

used as a reference. All samples were heated to a maximum temperature of 190 °C and cooled to a minimum temperature of −20 °C at a rate of 10 °C/min. TRIOS 5.1.1 software (TA Instruments, New Castle, DE) was used to analyze the melting, crystallization, and thermal degradation temperatures of each sample. Thermal analyses were performed for only one representative sample of each treatment.

Migration of PP-g-Cur Polymer in Food Simulants. The migration of curcumin into food simulants was analyzed using a method based on recommendations from the FDA[39] and EU.[40] Sample coupons (2 cm^2) were placed in glass headspace vials along with 10 mL of food simulant. The simulants used were deionized water (aqueous foods), 3% acetic acid (acidic foods), 10% ethanol (low alcohol foods), 50% ethanol (lipophilic foods), and 95% ethanol (fatty foods) to represent a range of applications. Each headspace vial was sealed with a polytetrafluoroethylene-butyl (PTFE-butyl) septum and crimp-top aluminum seal and incubated at 40 °C for 10 days. After incubation, aliquots were taken from each vial and analyzed on a Synergy Neo2 Hybrid Multi-Mode Reader (BioTek Instruments, Winooski, VT) at 428 nm, which was experimentally determined to be the maximum absorbance wavelength for curcumin (Figure S4). The amount of curcumin migrated from each sample was determined by comparison to curcumin standard curves made in each food simulant, with each food simulant acting as the respective blank. All standard curves were made in triplicate using a stock solution of 0.1 mg/mL curcumin in absolute ethanol that was diluted into each simulant. The amount of curcumin migration was compared to the limit of migration for packaging constituents listed by the European Union (10 mg/100 cm^2).[40] Migration analysis was performed in quadruplicate for each of two independently extruded batches of each treatment.

UV and Visible Light Transmission. The UV-barrier and visible light transmission properties of control and treated films were analyzed using a method adapted from Roy et al.[41] Polymer samples were hole-punched using a standard hand-held 1/4 in. hole puncher and placed in a clear-bottomed 96-well plate. The absorbance of each sample was analyzed from 280 to 800 nm with 2 nm resolution on a Synergy Neo2 Hybrid Multi-Mode Reader (BioTek Instruments, Winooski, VT). The absorbance values of blank wells were subtracted from sample absorbance values, which were then converted to percent transmission and plotted against wavelength. Optical analysis was averaged from two independent coupons from two independently extruded batches (totaling four replicates per treatment).

Demonstrating the Intelligent and Active Properties of PP-*g*-Cur. *Radical Scavenging Assays.* The antioxidant performance of control and treated polymers was determined using 2,2-diphenyl-1-picrylhydrazyl radical (DPPH·) and 2,2′-azino-bis(3-ethylbenzothiazoline-6-sulfonic acid) (ABTS·+) assays adapted from previous work.[41] The DPPH assay was performed by incubating 1 × 1 cm^2 coupons in 0.5 mL of DPPH solution (0.1 mM in ethanol) mixed with 0.5 mL of ethanol in a 24-well plate. Coupons were incubated for 24 h at 25 °C in the dark with shaking at 150 rpm. After incubation the absorbance of each solution was read on a Synergy Neo2 Hybrid Multi-Mode Reader (BioTek Instruments, Winooski, VT) at 517 nm and compared against a Trolox standard curve (0−40 μM) in ethanol. For the ABTS assay, a 1:1 volumetric mixture of 7 mM ABTS in 4 mM sodium phosphate buffer (pH 7.4, adjusted with hydrochloric acid and sodium hydroxide) and 2.45 mM potassium persulfate in sodium phosphate buffer, pH 7.4, was reacted for 16 h in the dark at room temperature (~20 °C) to create the radical stock solution. The stock solution was diluted with either ethanol or 4 mM sodium phosphate buffer (pH 7.4) (organic and aqueous, respectively) to an absorbance of 0.900 ± 0.30 at 734 nm to produce the ABTS working solution. In a 24-well plate, 1 × 1 cm^2 coupons of each film were incubated with 0.5 mL of organic ABTS working solution and 0.5 mL of ethanol or 0.5 mL of aqueous ABTS working solution and 0.5 mL of 4 mM sodium phosphate buffer (pH 7.4) for organic and aqueous ABTS assays, respectively. The plate was incubated at 30 °C for 4 h for the organic solution and 24 h for the aqueous solution. The absorbance of each well was analyzed on a Synergy Neo2 Hybrid Multi-Mode Reader (BioTek Instruments, Winooski, VT) at 734 nm and converted to TEAC using a Trolox standard curve (0−40 μM)

https://doi.org/10.1021/acsami.3c06589
ACS Appl. Mater. Interfaces 2023, 15, 29511−29524

made in either ethanol or 4 mM sodium phosphate buffer (pH 7.4). For both the DPPH and ABTS assays, the average Trolox equivalent antioxidant capacity (TEAC) of the blank wells (containing no coupons) was subtracted from the TEAC values of each sample to account for any color degradation of the DPPH or ABTS solution during incubation. ABTS assays were performed in duplicate on quadruplicate coupons from each of two independently extruded batches of each treatment (totaling 16 replicates per treatment), and DPPH assays were performed in duplicate on triplicate coupons from each of two independently extruded batches of each treatment (totaling 12 replicates per treatment). Sample sizes for the DPPH and ABTS samples were determined independently to enable equivalent power for subsequent statistical analyses.

Accelerated Ascorbic Acid Degradation Assay. The ability of treated and control PP to inhibit the oxidative degradation of ascorbic acid was quantified using a method adapted from previous work.[20] In brief, 1 × 1 cm^2 coupons of each sample were incubated in glass GC vials with aluminum septum caps. The vials were filled with 1 mL of 20 mM ascorbic acid in 10 mM sodium acetate imidazole buffer (pH 4.0, adjusted with HCl) and incubated for 9 days at 37 °C. Concentration of ascorbic acid was measured on days 1, 3, 5, 7, and 9 using a modified version of the Association of Official Analytical Chemists method 967.21.38.[42] Aliquots of 20 μL from each vial were combined with 480 μL of 0.04 wt % oxalic acid (in water) in 1 mL Eppendorf tubes and vortexed until well mixed. Aliquots of 30 μL from this solution were combined with 470 μL of 0.2 mM dichloroindophenol (in water) in 1 mL Eppendorf tubes and vortexed until well mixed. The absorbance of the dichloroindophenol mixtures was immediately measured on a Synergy Neo2 Hybrid Multi-Mode Reader (BioTek Instruments, Winooski, VT) at 520 nm and converted to ascorbic acid concentrations using an ascorbic acid standard curve (0−20 mM). The ascorbic acid concentration of each sample over time was fit with a single-phase decay model. The assay was performed on quadruplicate coupons from two independently extruded batches, totaling eight replicates per treatment.

Antibacterial Properties. The Japanese Industrial Standard (JIS) Z2801:2000 method was slightly modified to analyze antibacterial activity of treated films against food-borne pathogenic bacteria.[43] Briefly, a culture of *E. coli* ATCC strain no. 25922 and a culture of *L. monocytogenes* from a food isolate were stored in 20% glycerol at −80 °C until use. The *L. monocytogenes* strain was obtained from the Cornell Food Safety Laboratory Bacterial Strains Collection as FSL C1-0053 and originally isolated from a finished ready-to-eat dairy food product. The cultures were streaked on tryptic soy agar (TSA) and incubated at 37 °C for *E. coli* and 30 °C for *L. monocytogenes* for 24 h. An isolated colony from each plate was used to inoculate 12 mL of tryptic soy broth (TSB), which was incubated with shaking for 24 h at 37 °C. A 100 μL aliquot of each culture was used to inoculate 50 mL of TSB, which was incubated with shaking for 24 h at 37 °C to achieve a cell density of 10^9 CFU/mL, which was confirmed by plate count on TSA. Each culture was diluted to reach a starting concentration of 10^5 CFU/mL, also confirmed by plate count on TSA. Treated films were cut into 5 × 5 cm^2 squares and stored in sterile conditions after the ethanol wash described in the synthesis step. A 0.4 mL aliquot of each 10^5 CFU/mL culture was placed on the treated films and covered with a 4 × 4 cm^2 sterile PP film to create a sandwich. The PP cover was lightly pressed down with sterile tweezers to distribute the inoculum across the treated film, and the sandwich was placed in a Petri dish. The Petri dish was placed in an airtight box containing paper towels saturated with 100 mL of filtered water to maintain a humid environment. The entire apparatus was incubated at 37 °C for 24 h. After incubation, 10 mL of phosphate buffered saline (PBS, pH 7.4) solution was pipetted into each Petri dish and well mixed to disassemble the sandwich and dilute the inoculated broth. An aliquot was taken from each Petri dish and serially diluted with PBS buffer. A 100 μL aliquot of the appropriate dilution was plated in duplicate on TSA and incubated for 24 h at 37 °C. Plates with 30−300 CFU were counted, and the average plate count of the duplicate plates was recorded. Plate counts for treated films were subtracted from the average plate count of the control to determine inhibition of bacterial growth. The assay was performed on triplicate coupons from two independently extruded batches, totaling six replicates per treatment.

To determine the antimicrobial performance of free curcumin, the assay was repeated with curcumin powder added to the starting inoculum. Curcumin powder was first completely dissolved in ethanol to prepare 2.0 and 0.2 mg/mL stock solutions. Stock solutions were diluted 10× in TSB to final concentrations of 200 and 20 μg/mL curcumin, which was then inoculated to a 10^5 CFU/mL starting concentration of either *E. coli* or *L. monocytogenes*, confirmed by plate count. The procedure was repeated by replacing the curcumin stock solutions with absolute ethanol (10% v/v in TSB) to quantify any growth inhibition due to ethanol. A 0.4 mL aliquot of each 10^5 CFU/mL starting inoculum was placed on 5 × 5 cm^2 sterile PP films and covered with a 4 × 4 cm^2 sterile PP film to create a sandwich, and the assay was repeated as described above. The assay on free curcumin powder was performed in triplicate for each stock solution.

Color Changing Response to Ammonia Vapor. The color changing properties of treated films were demonstrated using a method adapted from previous work.[29,30] Films were cut into 1.3 × 1.3 cm^2 coupons and attached to the inside of PTFE-butyl septa using Kapton double-sided tape. The septa were placed in aluminum caps and crimped to 10 mL glass headspace vials filled with 9 mL of 0.8 mM ammonia. Coupons were left to incubate at room temperature (22 °C) for 24 h. After incubation the coupons were removed from the septa and immediately analyzed with a CR-400 Chroma Meter (Konica Minolta Sensing, Ramsey, NJ) using CIELab color space parameters. The color space parameters of the coupons prior to ammonia exposure were also recorded. The total color change (ΔE^*, eq 1) and the chromatic parameter (ΔC^*, eq 2) of each treated film were calculated

$$\Delta E^* = \sqrt{(L^*_1 - L^*_2)^2 + (a^*_1 - a^*_2)^2 + (b^*_1 - b^*_2)^2} \quad (1)$$

$$\Delta C^* = \sqrt{(a^*_1 - a^*_2)^2 + (b^*_1 - b^*_2)^2} \quad (2)$$

where L^* represents lightness, a^* represents redness/greenness, and b^* represents blueness/yellowness. Digital photographs of each coupon were taken in a light box before and after incubation to show visible color change. This assay was performed on triplicate coupons from two independently extruded batches, totaling six replicates per treatment. Images presented in the results were randomly selected using a random number generator across replicates, and a square crop of each photo was taken to maximize the area shown.

Statistical Analysis. Extrusion of all films was performed in duplicate batches on two independent days, and all results are equally representative of both batches. All data was analyzed for normality using the Shapiro−Wilk test on GraphPad Prism 9.3.0 (La Jolla, CA). Statistical significance for water contact angle, color change response to ammonia, radical scavenging assays, and antibacterial properties was analyzed using analysis of variance (ANOVA) with Tukey's HSD multiple comparisons ($p < 0.05$). Statistical significance for the migration assay was analyzed using ANOVA with Dunnett's HSD compared to control PP on GraphPad Prism 9.3.0 (La Jolla, CA). Migration data for 50% EtOH and 95% EtOH simulants followed a log-normal distribution, so ANOVA with Dunnett's HSD was performed on the log values for those simulants to determine statistical significance.

RESULTS AND DISCUSSION

Synthesis of Antioxidant Polypropylene (PP-*g*-Cur). Peroxide-initiated radical grafting reactions are one of the most common strategies used to modify PP to increase material compatibility, adhesion, and functionalization.[44] The reaction begins by the thermal decomposition of the peroxide into alkoxy radicals, which subsequently abstract a hydrogen from the tertiary carbon of the PP and a phenolic or carbon-centered hydrogen at the β-diketone from the curcumin to

https://doi.org/10.1021/acsami.3c06589
ACS Appl. Mater. Interfaces 2023, 15, 29511−29524

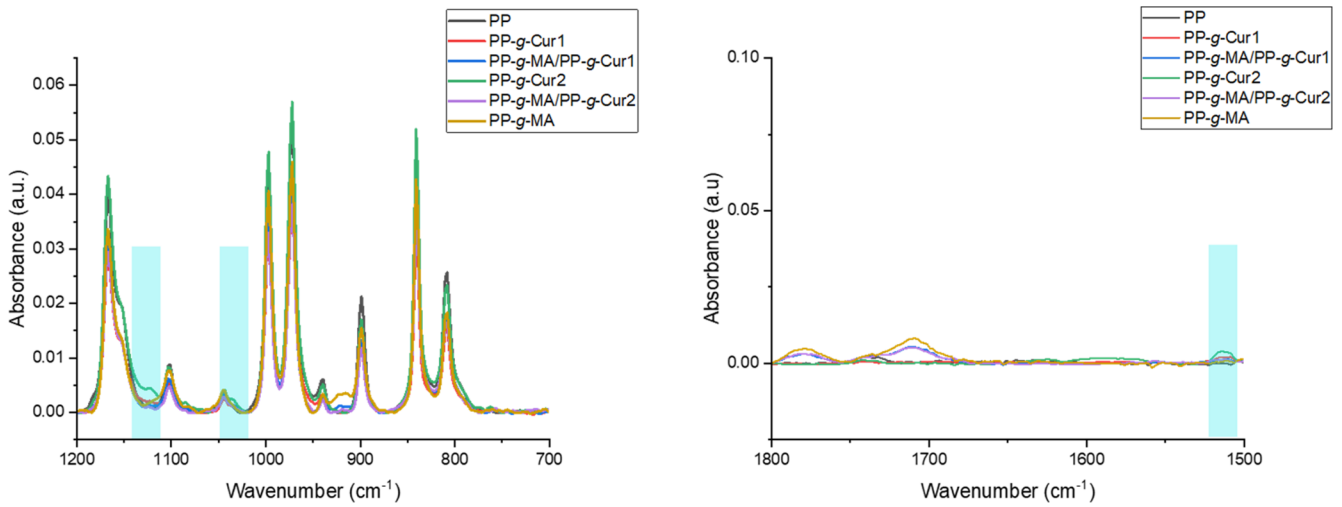

Figure 1. ATR-FTIR spectra of control and treated films. Characteristic PP alkyl bands are represented along with highlighted bands characteristic of curcumin's aromatic ring (left). PP-*g*-MA carboxylic acid and anhydride carbonyl bands are shown, and curcumin ethylene bands are highlighted (right).

form a macroradical.[16] According to previous research, the phenoxy radical on the curcumin can undergo an intermolecular radical transfer process that shifts the radical to the ortho or para position relative to the hydroxyl.[31,35,36] The carbon-centered radical at the *β*-diketone moiety will also undergo an intermolecular radical transfer to form an enolic alkoxy radical.[37] The aromatic or alkoxy radical on the curcumin can then react with the PP macroradical to form the grafted product. The proposed mechanism and potential functionalized products are outlined in Scheme 1.

The temperature profile of the extruder was designed to optimize the grafting reaction. According to TGA and DSC analysis (Figure S3), curcumin melts at 177 °C and decomposes at 205 °C, whereas PP melts at 160 °C and does not decompose until above 400 °C. To prevent immediate quenching of the radical initiator by curcumin, a radical scavenger, the first two mixing zones were set to 160 and 165 °C to melt only DCP and PP. Therefore, in these initial mixing zones, curcumin was conveyed and mixed with the polymer and initiator in the extruder as a solid powder. Unmelted curcumin can only react on the surface of the solid particles, resulting in minimal reactivity with the DCP radicals. Thus, keeping the initial mixing zones at low temperature allows decomposition of DCP and formation of PP macroradicals while minimizing quenching by curcumin. The final mixing zone was set to 175 °C to melt curcumin, increasing interaction and thus reactivity with the PP and DCP radicals. Temperatures were kept close to the reactant melting temperatures to account for frictional heat[45] and prevent degradation of curcumin due to high temperatures and shear.[46]

Preliminary experiments were performed with 0.1% and 0.5% w/w DCP concentration, and results showed improved immobilization and optical properties of films using 0.5% w/w DCP. Higher concentrations of initiator were not tested based on previous literature demonstrating the degradation of PP mechanical properties as a direct result of increasing DCP concentration.[47] Curcumin concentration of 3% w/w was also tested, but ABTS radical scavenging assay showed no improvement in antioxidant performance over 2% w/w curcumin samples, and discrete particles of curcumin could be seen in the film, indicating saturation. For these reasons, only 1% and 2% w/w curcumin samples were used in subsequent experiments.

Curcumin is a hydrophobic compound with low water solubility, which limits its functional performance in aqueous environments. PP-*g*-MA has often been used as a hydrophilic compatibilizer in PP blends to improve homogenization by preventing aggregate formation of additives and macromolecules.[48] We thus hypothesized that the compatibilization of PP-*g*-MA with PP base polymer would improve interactions between the active polymer and aqueous food matrices, thus expanding the range of foods and beverages with which this active material could perform well. Additionally, PP-*g*-MA contains both anhydride and carboxylic acid groups, which can interact with the ketone and phenol groups in curcumin to improve miscibility and enhance optical and interfacial properties of the polymer. Thus, studies were performed on both PP-*g*-Cur films as well as PP-*g*-Cur/PP-*g*-MA copolymer films to observe the effects of a compatibilizer on material properties and functionality.

Characterizing the Interfacial, Chemistry, Thermal, and Optical Properties of PP-*g*-Cur. The presence of curcumin in sample films was confirmed by ATR-FTIR (Figure 1). The absorbance band at 1510 cm^{-1} was attributed to the C=C vibration in curcumin,[49] the band at 1122 cm^{-1} correlates to the C−O stretching of curcumin on the aromatic ring, and the band at 1035 cm^{-1} indicates the C−C stretching of curcumin on the aromatic ring.[41] These characteristic curcumin absorbance bands are only visible in the PP-*g*-Cur2 films, likely due to this sample having the highest concentration of curcumin. Other films containing <2% w/w curcumin are likely below the threshold of detection for ATR-FTIR. Spectra of films containing MA have absorbance at 1778 and 1710 cm^{-1}, representing carbonyl C=O stretching characteristic of the anhydride and carboxylic acid groups, respectively.

Dynamic water contact angle was performed to characterize the hydrophobicity and interfacial behavior of the treated films (Table 2). The advancing contact angle (θ_A) analysis was performed by depositing a water droplet on the film surface, expanding the droplet at a constant rate, and recording the maximum contact angle before the baseline of the droplet

https://doi.org/10.1021/acsami.3c06589
ACS Appl. Mater. Interfaces 2023, 15, 29511−29524

Table 2. Dynamic Water Contact Angle of Treated and Control Films Including Advancing Contact Angle, Receding Contact Angle, and Hysteresis[a]

sample	advancing (θ_A)	receding (θ_R)	hysteresis (θ)
PP	116.5 ± 2.0^{A}	94.3 ± 1.9^{A}	22.1 ± 2.8^{A}
PP-*g*-MA/PP	120.4 ± 3.9^{AB}	46.5 ± 4.2^{B}	73.9 ± 5.5^{B}
PP-*g*-Cur1	120.2 ± 8.1^{AB}	75.4 ± 9.4^{C}	44.8 ± 3.0^{C}
PP-*g*-MA/PP-*g*-Cur1	126.5 ± 4.9^{BC}	50.4 ± 3.4^{B}	76.1 ± 6.4^{B}
PP-*g*-Cur2	125.7 ± 2.8^{BC}	74.8 ± 7.0^{C}	50.9 ± 5.9^{C}
PP-*g*-MA/PP-*g*-Cur2	130.8 ± 5.3^{C}	49.5 ± 5.8^{B}	81.2 ± 6.5^{B}

[a]Values are the average and standard deviation of two different spots of two different coupons from two independently extruded batches of each sample. Significant differences between means in each column are signified by different uppercase superscript letters (Tukey's HSD, $p \leq 0.05$).

increases. The receding contact angle (θ_R) was produced similarly, but by decreasing the water droplet size and recording the contact angle prior to the baseline decreasing. Hysteresis is the difference between advancing and receding contact angle and gives an indication of the chemical heterogeneity of the films surface. All films displayed hydrophobic advancing contact angles (defined as $\theta_A > 90°$, with all films here presenting $\theta_A > 115°$), which indicates the desirable low wettability of PP packaging was maintained across all treated samples. Compared to control PP, samples containing curcumin had increased advancing contact angle, likely due to the hydrophobic nature of curcumin. A similar trend was seen by Tsekova et al. when the water contact angle of hydrophobic cellulose acetate (123.10 ± 2.0°) increased with the addition of curcumin (129.4 ± 3.8°).[50] The compatibilization of PP-*g*-Cur with PP-*g*-MA further increased the advancing contact angle, likely due to the improved miscibility of the films due to hydrogen-bonding interactions between MA carboxylic acids and curcumin. It has been shown in previous studies that improved miscibility can decrease surface free energy, which increases the advancing contact angle of a polymer.[51] This result emphasizes the utility of PP-*g*-MA as a compatibilizer to improve the interfacial properties of the novel material.

Receding contact angles were significantly different between treated and control films. Samples containing MA had the lowest receding contact angles, likely due to the hydrogen bonding of the MA carboxylic acids to water, which increases interaction of the water droplet with the film. PP-*g*-Cur1 and PP-*g*-Cur2 exhibited larger receding contact angles than polymers with PP-*g*-MA, as can be expected due to the hydrophobic nature of PP and curcumin. Because interaction of the active packaging material with aqueous food matrices is important to enable preservative activity, these results once again emphasize the importance of PP-*g*-MA not only as a compatibilizer within the polymer but also between the polymer and food matrix. Compared to control PP, PP-*g*-Cur1 and PP-*g*-Cur2 displayed lower receding contact angles, potentially due to the immiscibility and aggregation of curcumin that increases surface roughness of the films.[52] These results suggest desirable surface orientation of the active ligand, which would increase chemical heterogeneity of the sample films, as demonstrated by the increasing hysteresis values. Overall, lower receding contact angles of sample films compared to control PP signifies improved interaction between the functional material and aqueous food matrix, which would support the ability of the active packaging material to impart preservative functionality on packaged foods or beverages.

TGA and DSC were performed to characterize the thermal stability and properties of the treated films (Figure S3). Although curcumin powder decomposes at much lower temperatures than PP, no additional decomposition steps were observed in any of the samples, likely due to the low concentrations of MA and curcumin compared to PP. PP-*g*-Cur2 and PP-*g*-MA/PP-*g*-Cur2 samples showed slightly lower thermal stability, likely due to the disruption of PP crystallinity by curcumin and MA. DSC spectra showed melting temper-

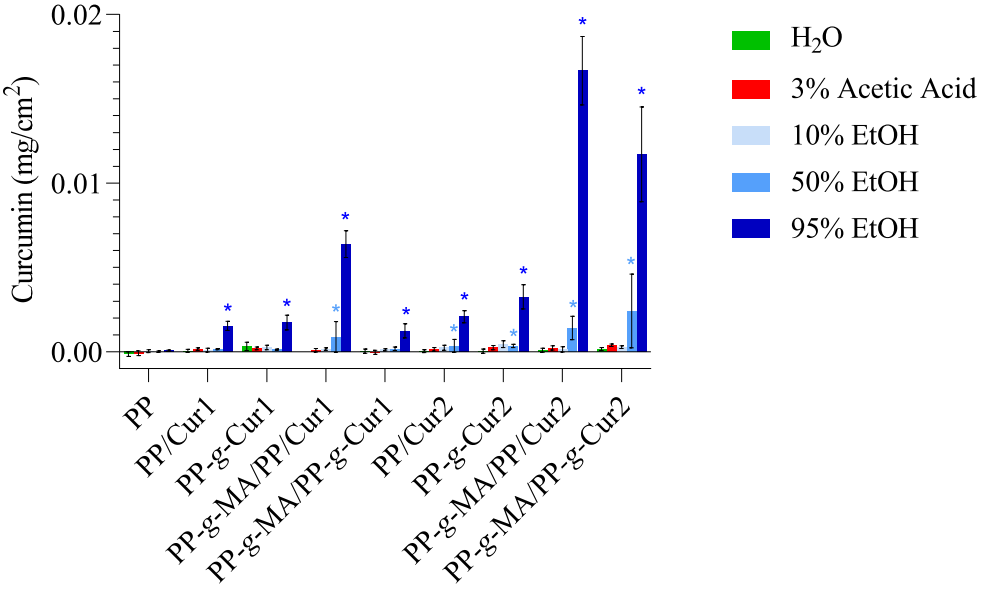

Figure 2. Migration study of treated and control films at 40 °C for 10 days in water, 3% acetic acid, 10% EtOH, 50% EtOH, and 95% EtOH. All films had curcumin migration significantly below the EU migratory limit for food contact materials (0.1 mg/cm^2). Values are the average and 95% confidence intervals of four replicates for each of two independently extruded batches. Statistically significant differences between the mean of each sample compared to the mean of PP for each simulant are signified by color-coded asterisks (Dunnett's HSD, $p \leq 0.05$).

https://doi.org/10.1021/acsami.3c06589
ACS Appl. Mater. Interfaces 2023, 15, 29511−29524

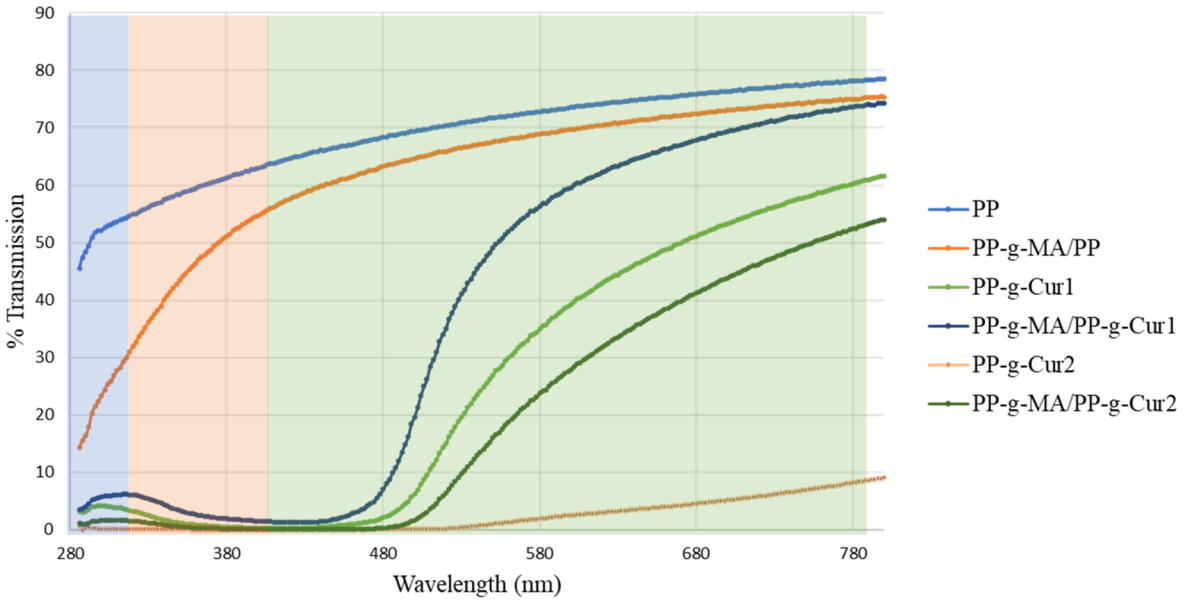

Figure 3. UV−vis spectrophotometry spectra (280−800 nm) of treated and control films to demonstrate UV blocking and visible light transmission of treated films. UV-B, UV-A, and visible light spectra are indicated by blue, orange, and green highlighting, respectively. Absorbance measurements were taken every 2 nm for two replicates from each of two independently extruded. Points shown are the average of all replicates for each sample.

atures of 160 °C for control PP, 159 °C for control PP-*g*-MA/PP, and 157 °C for all sample films. This minor decrease in thermal stability for sample films can be explained by the heterogeneity of the polymer chain with the introduction of MA and curcumin and by the lower molecular weight of the PP base polymer caused by beta scission during radical grafting.[53] The crystallization temperatures of PP-*g*-MA/PP, PP-*g*-MA/PP-*g*-Cur1, and PP-*g*-MA/PP-*g*-Cur2 were 120, 118, and 118 °C, respectively, compared to PP crystallization temperature of 116 °C. This increase in crystallization temperature of films containing PP-*g*-MA can be explained by previous studies that demonstrated how small amounts of MA can act as nucleating agents in PP to facilitate crystallization.[54] Despite these minor differences between control and sample films thermal properties, DSC and TGA analyses revealed no practically significant differences for sample films in food packaging applications, and thermoforming and heat sealing properties were unaffected by the radical grafting of curcumin.

Although curcumin is an approved food additive, the goal of this research was to immobilize curcumin to the polymer surface to impart active and spoilage-indicating functionality without affecting the quality or formulation of the packaged product. An accelerated migration study was performed based on EU[40] and FDA[39] recommendations for food contact materials to quantify the migration of curcumin from PP-*g*-Cur (Figure 2). Coupons of control and treated films were incubated in various food simulants for 10 days at 40 °C. After incubation, the concentration of curcumin was quantified using curcumin standard curves in each simulant (Figure S5). Water, 3% acetic acid, 10% ethanol (EtOH), 50% EtOH, and 95% EtOH represent aqueous, acidic, slightly alcoholic or slightly fatty, highly alcoholic, and highly fatty food environments, respectively.[39] Regardless of simulant, all sample films exhibited curcumin migration levels significantly below the migratory limit established by the EU for food contact materials (0.1 mg/cm^2),[40] validating that PP-*g*-Cur and PP-*g*-MA/PP-*g*-Cur films can be used for nonmigratory packaging. Indeed, depending on the simulant, between 0 and 0.0117 mg/cm^2 of curcumin migrated, the maximum of which is 8.5 times lower than the EU limit. For water, 3% acetic acid, and 10% EtOH, there was no migration of curcumin across any of the treated films compared to PP. Only films containing both PP-*g*-MA and Cur2 exhibited statistically significant migration in 50% EtOH, likely due to the hydrogen-bonding interactions between the simulant and MA that facilitates better contact with the material. Almost all films showed statistically significant migration in the 95% EtOH simulant, which is expected as EtOH is the best solvent for curcumin extraction.[55] It is worth noting, however, that PP-*g*-MA/PP-*g*-Cur1 films exhibited less than a fifth the curcumin migration in 95% EtOH as PP-*g*-MA/PP/Cur1 films, the only difference being the addition of DCP to radically graft curcumin to PP. This result supports the covalent grafting of curcumin to PP during reactive extrusion. Thus, these materials show great potential as nonmigratory packaging, particularly for aqueous (beverages), acidic (condiments and juices), and slightly lipophilic (meats, seafood, sauces, and dressing) products.

UV−vis spectrophotometry was used to characterize the optical properties of PP-*g*-Cur films (Figure 3) based on previous work that demonstrated the UV-blocking capability of curcumin incorporated in migratory carboxymethyl cellulose active packaging.[41] UV light exposure can negatively affect components of food that are susceptible to oxidative degradation by free radicals, known as photosensitizers. These components include lipids, colorants, and vitamins and minerals that can significantly impact the appearance, flavor, texture, and nutritional value of the product. Thus, it is of critical importance to reduce the UV degradation of packaged foods.[56] However, ideal packaging materials would also retain the high visible light transmission of native PP, which allows consumers and manufacturers to see the packaged product. A spectral sweep of treated and control films revealed significant blocking in the UV-B (280−315 nm)

https://doi.org/10.1021/acsami.3c06589
ACS Appl. Mater. Interfaces 2023, 15, 29511−29524

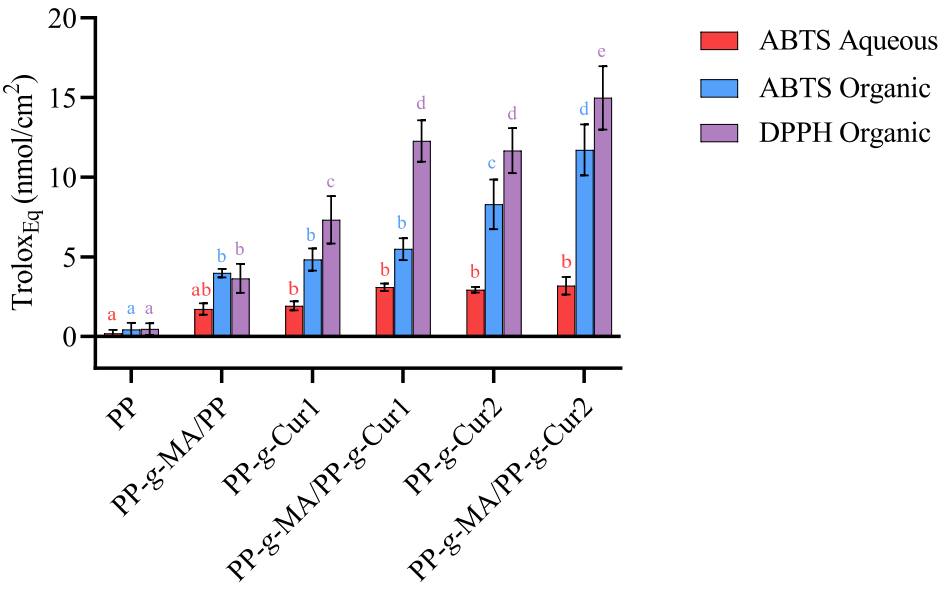

Figure 4. ABTS and DPPH radical scavenging assay of control and treated films to demonstrate antioxidant performance of PP-*g*-Cur films in different matrices. Values are the average and 95% confidence intervals of eight replicates (ABTS) and six replicates (DPPH) for each of two independently extruded batches of each treatment. Statistically significant differences between sample means for each assay are signified by color-coded letters (Tukey's HSD, $p \leq 0.05$).

and UV-A (315−400 nm) region and high transmission in the visible light region (400−700 nm).[41] For instance, PP-*g*-MA/PP-*g*-Cur1 blocked 93% of all UV light while allowing 64% visible light transmission compared to control PP. Blending with PP-*g*-MA significantly improved visible light transmission compared to films containing no compatibilizer. This difference is likely due to the hydrogen-bonding interactions between MA and curcumin that improve miscibility and homogenization, highlighting the importance of a compatibilizer in improving optical properties of the material. Compared to native PP and PP-*g*-MA, these films have high potential to prevent degradation of packaged products by UV light.

Demonstrating the Intelligent and Active Properties of PP-*g*-Cur. Oxidation of food is due to the formation of reactive oxygen species (ROS) caused by heat, enzymes, transition metals, and/or UV light, which can cause product discoloration, nutrient degradation, and rancidity.[6,9] Protection against oxidation is important in both organic and aqueous environments because ROS can cause lipid oxidation as well as degradation of proteins, vitamins, and sugars.[57] ABTS and DPPH Trolox equivalent antioxidant capacity (TEAC) assays were used to determine the antioxidant performance of PP-*g*-Cur films compared to control films because ABTS assays are typically used for hydrophilic and lypophilic antioxidant systems, and DPPH assays are typically used for hydrophobic antioxidant systems (Figure 4).[58] The colorimetric decrease of each solution signified sequestering of preformed radicals and was quantified using a standard curve of Trolox, which is the synthetic water-soluble analogue to Vitamin E. Across all assays, treated films showed significant antioxidant capacity compared to control PP, which had negligible TEAC values. PP-*g*-MA/PP-*g*-Cur2, displayed the highest TEAC values across all assays, with 3.18, 11.71, and 14.98 Trolox$_{Eq}$ (nmol/cm^2) for aqueous ABTS, organic ABTS, and organic DPPH, respectively. The aqueous ABTS assay displayed the lowest TEAC values for PP-*g*-Cur films, potentially due to the limited interaction between the hydrophobic material and aqueous environment. However, aqueous ABTS values are higher than those reported by other nonmigratory antioxidant active packaging studies with demonstrated efficacy in preventing oxidative degradation, such as PLA grafted with nitrilotriacetic acid (0.89 ± 0.07 Trolox$_{Eq}$ (nmol/cm^2))[20] and polyethylene grafted with fish peptide (~1.2 Trolox$_{Eq}$ (nmol/cm^2)).[59] The ABTS and DPPH assays performed in organic solvent showed significantly higher TEAC values across all treated films, likely due to the improved interactions between curcumin and EtOH as seen in the migration assay for 95% EtOH simulant. As EtOH is the preferred solvent for curcumin extraction, it can be assumed that EtOH would have significant hydrogen-bonding interactions with the grafted curcumin, improving interactions between the antioxidant films and free radicals in solution. In the organic ABTS assay, PP-*g*-Cur2 and PP-*g*-MA/PP-*g*-Cur2 films were the only samples with significant TEAC values compared to the control PP-*g*-MA/PP, likely due to the higher concentration of curcumin in PP-*g*-Cur2 and the increased polarity in PP-*g*-MA/PP-*g*-Cur2. DPPH showed slightly different results, with all samples performing between 2 and 4 times better than the PP-*g*-MA/PP control. In addition, this assay showed a synergistic effect between PP-*g*-Cur and PP-*g*-MA, where the TEAC value of PP-*g*-MA/PP-*g*-Cur films was higher than either of the polymers individually. For instance, TEAC values for PP-*g*-MA/PP and PP-*g*-Cur2 were 3.65 and 11.67 Trolox$_{Eq}$ (nmol/cm^2), respectively. PP-*g*-MA/PP-*g*-Cur2, which contains the same concentration of PP-*g*-MA as PP-*g*-MA/PP films and only half the concentration of curcumin as PP-*g*-Cur2 films, would be have an expected TEAC value of ~9.49 Trolox$_{Eq}$ (nmol/cm^2). However, the experimental TEAC value of PP-*g*-MA/PP-*g*-Cur2 was 14.98 Trolox$_{Eq}$ (nmol/cm^2), which shows a synergistic effect between PP-*g*-MA and curcumin. One explanation of this effect could be the hydrogen-bonding interactions between MA and curcumin, which could help to stabilize curcumin's anionic form. According to Litwinienko et al., curcumin scavenges DPPH radicals by sequential proton loss electron transfer (SPLET), in which the keto−enol moiety of curcumin becomes deprotonated in an ionizing solvent

https://doi.org/10.1021/acsami.3c06589
ACS Appl. Mater. Interfaces 2023, 15, 29511−29524

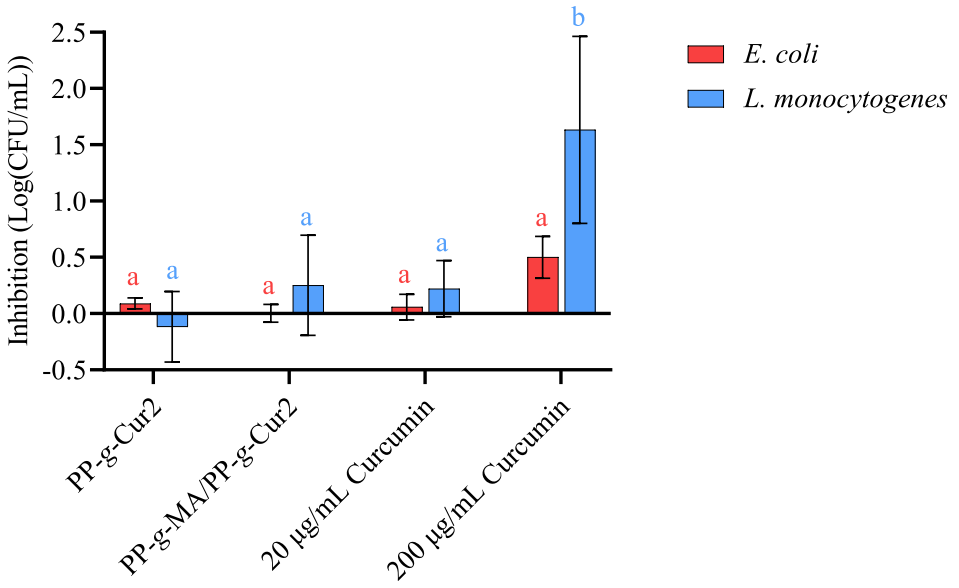

Figure 5. Bacterial growth inhibition assay to display the antibacterial performance of treated films and free curcumin. Results represent the log difference in plate counts between the control and treated samples. Values for treated films are the average and standard deviation of three replicates for each of two independently extruded batches of each treatment. Values for free curcumin are the average and standard deviation of three replicates. Statistically significant differences between sample means for each bacterial strain are signified by color-coded letters (Tukey's HSD, $p \leq 0.05$).

(EtOH), forming an anion that then transfers an electron to DPPH radicals.[60] Hydrogen bonding between curcumin and MA may accelerate the ionization of curcumin by stabilizing the anionic form, which would improve DPPH radical scavenging in organic conditions as observed here.

Treated and control films were tested in aqueous ABTS, organic ABTS, and organic DPPH assays to demonstrate the antioxidant properties and performance of PP-*g*-Cur films in different environments. The ABTS assay is often utilized to demonstrate antioxidant performance in lipophilic and hydrophilic systems, whereas the DPPH assay is standard for hydrophobic antioxidants such as polyphenols.[58] All assays displayed significant radical scavenging capacity of treated films, highlighting the applicability of PP-*g*-Cur as antioxidant packaging for both lipophilic and aqueous food systems. According to previous studies, curcumin scavenges both ABTS and DPPH radicals primarily by the SPLET mechanism.[60,61] Because this mechanism is dependent on the deprotonation of curcumin, the solvent plays a major role in the kinetics of curcumin radical scavenging. EtOH is an ionizing solvent that facilitates deprotonation of curcumin's enol moiety, which allows the SPLET mechanism to dominate the organic ABTS and DPPH assays. On the other hand, the aqueous assay is performed at pH 7.4, which is below the pK_a of the enolic hydrogen (pH 7.8).[62] Because curcumin is not deprotonated at this pH value, we hypothesize that the primary mechanism of aqueous ABTS radical scavenging is by hydrogen atom transfer (HAT) from curcumin's phenol moiety, which is significantly slower than the SPLET mechanism. As a result, it is possible a longer incubation time in the aqueous ABTS assay would yield higher radical scavenging results for curcumin; however, the instability of the ABTS radical at pH 7.4 limits the incubation time of this assay. Overall, these assays help to elucidate the mechanisms that dominate curcumin's radical scavenging performance in various environments.

Because previous research has highlighted the time dependence of radical scavenging assays, preliminary experiments were conducted to determine the optimal incubation time for measuring antioxidant performance of treated films (Figure S6). Previous studies have shown that traditional incubation times (between 5 and 30 min) underestimate the TEAC values of polyphenols due to the slow radical scavenging mechanisms.[63] The incubation time chosen for each assay was based on the highest TEAC value for PP-*g*-Cur films while the control radical solution (containing no film) maintained greater than 50% its initial absorbance value. ABTS and DPPH radicals are unstable, and the color of the solutions tends to degrade over time without radical scavenging by antioxidants. This instability is particularly true for ABTS solutions in EtOH or neutral/basic buffered aqueous systems, which are significantly less stable than acidic ABTS solutions (Figure S6). The ABTS and DPPH solutions were incubated without films throughout the time trial experiment to monitor when absorbance fell below 50% of the initial value, a level used by previous studies to indicate radical instability.[63] This restriction ensured that the observed decrease in absorbance was due to radical scavenging rather than radical instability. Results demonstrated radical scavenging performance of PP-*g*-Cur films increased significantly over time, which is relevant for food packaging applications which seek to improve shelf life over the course of days, weeks, or months. Without these preliminary experiments, traditional incubation times for ABTS and DPPH assays would have significantly underestimated the antioxidant capacity of treated films. This time trial data highlight the importance of understanding radical scavenging kinetics of different compounds to fully demonstrate their antioxidant performance.

An accelerated ascorbic acid degradation study was performed to demonstrate whether treated films provided protection against metal-catalyzed oxidation (Figure S7). Trace metals found in food and beverages such as copper and iron can accelerate oxidation and nuritent degradation,[6] which can be inhibited by the presence of metal chelators. Previous studies have demonstrated the chelating performance

https://doi.org/10.1021/acsami.3c06589
ACS Appl. Mater. Interfaces 2023, 15, 29511−29524

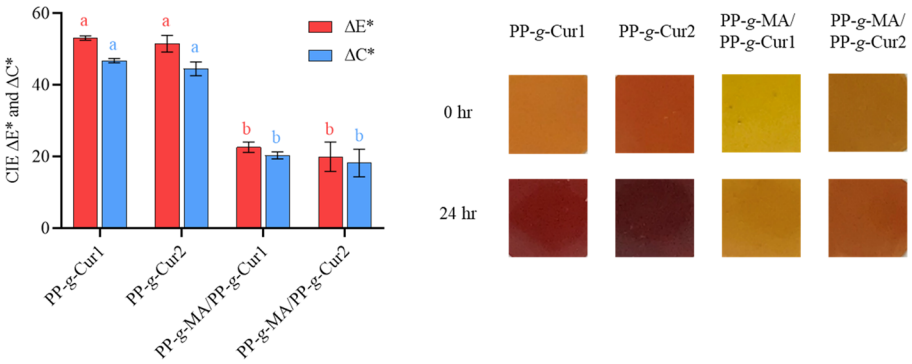

Figure 6. CIELab color change values of PP-*g*-Cur films to demonstrate quantifiable intelligent film properties in the presence of ammonia gas (left). Photographs of treated films before and after ammonia exposure to demonstrate visual color change for food applications to indicate spoilage to consumers and manufacturers (right). Values are the average and standard deviation of three replicates for each of two independently extruded batches. Statistically significant differences between sample means are indicated by color-coded letters (Tukey's HSD, $p \leq 0.05$).

of curcumin for therapeutic applications,[24] which primarily occur at physiological pH values. However, most food systems are acidic, particularly those that use ascorbic acid such as fruit, beverages, and condiments. In this assay, which was performed at pH 4.0 to represent typical food applications, treated films showed no protection against ascorbic acid degradation compared to control PP. Under neutral and acidic conditions the bis-keto form of curcumin is dominant, whereas under basic conditions the enolate form is dominant.[30] Because the metal chelating properties of curcumin are dependent on the anionic keto−enol complex, curcumin likely cannot chelate metals in acidic food applications, as demonstrated by these results.

Radical scavenging and ascorbic acid degradation results demonstrate the importance of interfacial properties in predicting and tailoring functional performance of active materials to specific applications. These experiments add to the growing body of knowledge concerning the mechanistic performance of natural active agents like curcumin. Importantly, while the films were not effective in preventing ascorbic acid degradation, significant radical scavenging capacity demonstrates their efficacy as nonmigratory antioxidant materials.

It is estimated that one-fourth of global food waste can be attributed to microbial spoilage,[64] which can cause off-odors, undesirable flavors, visible slimes and molds, and textural degradation that leads to consumer rejection and food waste. Previous work on curcumin migratory packaging has shown antibacterial efficacy against both Gram-negative and Gram-positive strains,[41,49] so treated films were tested against common food-borne pathogens *E. coli* and *L. monocytogenes* (Figure 5). Because treated films are nonmigratory, the Japanese Industrial Standard (JIS) Z2801:2000 method was used to ensure constant contact between the bacterial solution and films,[43] and only PP-*g*-Cur2 and PP-*g*-MA/PP-*g*-Cur2 films were used as they contain the highest concentration of curcumin. Previous studies reported the minimum inhibitory concentration (MIC) of curcumin to be between 100 and 200 μg/mL against *E. coli*,[65,66] so 20 and 200 μg/mL were chosen to represent curcumin concentrations below and above the reported MIC. None of the samples (aside from 200 μg/mL curcumin against *L. monocytogenes*) displayed any statistically significant antibacterial efficacy compared to the control. We hypothesize that the lack of antibacterial performance of PP-*g*-Cur2 films could be due to the limited interaction between the aqueous bacterial suspension and hydrophobic polymer. It was expected that copolymerization with PP-*g*-MA would improve active performance in aqueous matrices, but the PP-*g*-MA/PP-*g*-Cur2 film may not contain enough surface-oriented curcumin to be effective.

Antimicrobial activity of solutions of free curcumin were tested to determine whether the lack of antibacterial performance was due to the limitations of free curcumin or due to limitations of the treated films such as lack of surface orientation, insufficient curcumin concentration, polymer hydrophobicity, or steric hindrance due to grafting. The 20 μg/mL curcumin was fully solubilized in the bacterial suspension but did not display any antibacterial function, as expected because this concentration is significantly below the reported MIC. The 200 μg/mL solution of curcumin partially fell out of solution upon dilution in TSB but showed some efficacy against *L. monocytogenes* (1.63 ± 0.83 log(CFU/mL) inhibition), though not a practically significant effect to be relevant for food applications. Thus, even the maximum concentration of free curcumin that could be solubilized in the bacterial suspension demonstrated minimal antibacterial performance. These results highlight the challenge of using curcumin as an antimicrobial agent due to its extreme hydrophobicity and poor solubility, which is why recent efforts have focused on developing water-soluble curcumin, encapsulated curcumin, and curcumin nanoparticles for antimicrobial applications.[67] Overall, while it may be possible to slightly improve the antibacterial properties of films through higher concentrations of grafted curcumin or further hydrophilic modification, the hydrophobic properties of curcumin would likely limit any significant or practical antimicrobial behavior.

Microbial spoilage of meat and seafood results in the release total volatile basic nitrogen (TVBN) compounds that increase the alkalinity of the product. The phenolic hydroxyl groups of curcumin can become deprotonated upon exposure to alkaline conditions such as those produced by meat and seafood, changing the color of curcumin from yellow to red. Thus, curcumin has been explored for use as a spoilage indicator for packaged meat and seafood through visible color change.[25] Previous work involving curcumin intelligent packaging has demonstrated success using ammonia to replicate the release of TVBN by bacteria.[26,30] To test the color changing properties of PP-*g*-Cur films, sample coupons were exposed to ammonia for 24 h and analyzed using a colorimeter (Figure 6). To correlate color change values to visual observation, photo-

https://doi.org/10.1021/acsami.3c06589
ACS Appl. Mater. Interfaces 2023, 15, 29511−29524

graphs of samples were taken before and after incubation. The ΔE^* values observed for all treated films were similar to values observed by Cvek et al. when curcumin-blended poly(lactic acid)/poly(propylene carbonate) packaging was exposed to ammonia. This group also demonstrated the ability of the material to detect shrimp spoilage for intelligent packaging applications,[29] suggesting the PP-*g*-Cur films reported here maybe be capable of these applications as well. The ΔC^* values for PP-*g*-Cur films were reported to emphasize that the primary color change of all films was from yellow to red. Photographs demonstrate the visible color change of the films, which is important as a qualitative visual indicator to customers and manufacturers of food spoilage. Films containing PP-*g*-MA showed a decrease in color change compared to films without PP-*g*-MA, possibly due to the interaction of PP-*g*-MA with ammonia. The carboxylic acids present in PP-*g*-MA have a lower pK_a than that reported for the phenolic hydroxyls in curcumin, which could result in partial quenching of the ammonia.[38,62] In addition to demonstrating the application of this material as intelligent packaging, these results support that curcumin was not degraded during extrusion because possible degradation products such as ferulic acid and 4-vinyl guaiacol are incapable of this color change.[46]

CONCLUSION

In this work reactive extrusion, a scalable, efficient, and continuous process, was used to develop nonmigratory active and intelligent packaging to reduce food waste. The thermal stability and hydrophobicity of native PP were retained in treated films, and the maximum curcumin migration from PP-*g*-Cur material was confirmed to be less than one-fifth the EU migratory limit. Treated films maintained 64% transparency while blocking 93% of UV light, which could prevent photodegradation of packaged goods while retaining product visibility. Ascorbic acid degradation and radical scavenging assays demonstrated that the antioxidant behavior of these films is due to radical scavenging rather than metal chelating functionality. Results from ABTS and DPPH assays and time trials supported the SPLET antioxidant mechanism of curcumin in ionizing solvent (EtOH) and the HAT antioxidant mechanism of curcumin in nonionizing solvent (aqueous, pH 7.4). These results also highlighted the significance of radical scavenging kinetics in analyzing different compounds, particularly polyphenols and other natural antioxidants whose slow scavenging mechanisms may result in significant underestimation of performance under short incubation times. PP-*g*-Cur films were tested against both Gram-positive and Gram-negative bacteria but revealed no antibacterial functionality compared to control PP. Antibacterial analysis of free curcumin highlighted the challenges of using curcumin in aqueous applications due to its extremely low solubility and high hydrophobicity, which could limit bacterial inhibition by PP-*g*-Cur films. Finally, exposure to ammonia gas changed the color of treated films both visually and quantitatively, demonstrating the ability of these films to act as intelligent packaging to indicate spoilage of meat and seafood products.

Results of this project demonstrate, for the first time, immobilization of a multifunctional preservative and indicating compound (curcumin) through a single-step, solvent-free process, which can be adapted to a range of other thermoplastic polymers and polyphenolic compounds with applications beyond food. Full characterization of the material's mechanical properties and determination of its performance under conditions of intended use would be necessary steps in identifying appropriate commercial applications of the materials. This work presents not only a nonmigratory packaging material to reduce food loss and waste but also a method to advance the capabilities and commercial viability of functional materials. Furthermore, results from this project emphasize the importance of systematic applications-driven method development, such as in antioxidant or antibacterial assays, to highlight the true capacity and limitations of materials in real application environments.

ASSOCIATED CONTENT

Supporting Information

The Supporting Information is available free of charge at https://pubs.acs.org/doi/10.1021/acsami.3c06589.

Full FTIR spectra of treated and control films; TGA thermogram of treated and control films; DSC thermograms of treated and control films; UV−vis spectral sweep of curcumin solution; standard curves of curcumin in migration assay food simulants; ABTS and DPPH time trials and radical stability; and accelerated ascorbic acid degradation assay (PDF)

AUTHOR INFORMATION

Corresponding Author

Julie M. Goddard − *Department of Food Science, 365 Stocking Hall, Cornell University, Ithaca, New York 14853, United States;* orcid.org/0000-0002-3644-0732; Email: goddard@cornell.edu

Authors

Halle N. Redfearn − *Department of Food Science, 365 Stocking Hall, Cornell University, Ithaca, New York 14853, United States;* orcid.org/0000-0002-6086-413X

Matthew K. Warren − *Department of Food Science, 365 Stocking Hall, Cornell University, Ithaca, New York 14853, United States*

Complete contact information is available at: https://pubs.acs.org/10.1021/acsami.3c06589

Author Contributions

H.R.: conceptualization, data curation, formal analysis, investigation (lead), methodology, project administration, supervision, validation, visualization, writing - original draft preparation, writing - review and editing. M.K.W.: investigation (supporting), writing - review and editing (supporting). J.M.G.: conceptualization, funding acquisition, project administration, supervision, writing - review and editing.

Notes

The authors declare no competing financial interest.

ACKNOWLEDGMENTS

This work was supported by Awards 2019-68015-29230 and 2019-38420-28975 from the U.S. Department of Agriculture National Institute of Food and Agriculture. This work made use of the Cornell Center for Materials Research Shared Facilities which are supported through the NSF MRSEC program (DMR-1719875). This work was performed in part at the Cornell NanoScale Facility, an NNCI member supported by NSF Grant NNCI-2025233. The authors thank Cornell Statistical Consulting Unit for their support in statistical

experimental design and data analysis. The graphical abstract image was prepared with BioRender.com.

REFERENCES

(1) FDA. Food Loss and Waste, 2021. Available from: https://www.fda.gov/food/consumers/food-loss-and-waste.

(2) Petruzzi, L.; Corbo, M. R.; Sinigaglia, M.; Bevilacqua, A. Chapter 1 - Microbial Spoilage of Foods: Fundamentals. In *The Microbiological Quality of Food*; Bevilacqua, A., Corbo, M. R., Sinigaglia, M., Eds.; Woodhead Publishing: 2017; pp 1−21.

(3) FDA. Food Irradiation: What You Need to Know, 2018. Available from: https://www.fda.gov/food/buy-store-serve-safe-food/food-irradiation-what-you-need-know.

(4) Snyder, A. B.; Worobo, R. W. The Incidence and Impact of Microbial Spoilage in the Production of Fruit and Vegetable Juices as Reported by Juice Manufacturers. *Food Control.* **2018**, *85*, 144−50.

(5) Eneroth, Å; Christiansson, A.; Brendehaug, J.; Molin, G. Critical Contamination Sites in the Production Line of Pasteurised Milk, with Reference to the Psychrotrophic Spoilage Flora. *International Dairy Journal.* **1998**, *8* (9), 829−34.

(6) Gómez-Estaca, J.; López-de-Dicastillo, C.; Hernández-Muñoz, P.; Catalá, R.; Gavara, R. Advances in Antioxidant Active Food Packaging. *Trends in Food Science & Technology.* **2014**, *35* (1), 42−51.

(7) Yildirim, S.; Röcker, B.; Pettersen, M. K.; Nilsen-Nygaard, J.; Ayhan, Z.; Rutkaite, R.; et al. Active Packaging Applications for Food. *Comprehensive Reviews in Food Science and Food Safety.* **2018**, *17* (1), 165−99.

(8) Liu, F.; Antoniou, J.; Li, Y.; Yi, J.; Yokoyama, W.; Ma, J.; et al. Preparation of Gelatin Films Incorporated with Tea Polyphenol Nanoparticles for Enhancing Controlled-Release Antioxidant Properties. *J. Agric. Food Chem.* **2015**, *63* (15), 3987−95.

(9) Bastarrachea, L. J.; Wong, D. E.; Roman, M. J.; Lin, Z.; Goddard, J. M. Active Packaging Coatings. *Coatings* **2015**, *5* (4), 771.

(10) Goddard, J. M.; Talbert, J. N.; Hotchkiss, J. H. Covalent Attachment of Lactase to Low-Density Polyethylene Films. *J. Food Sci.* **2007**, *72* (1), No. E036.

(11) Lin, Z.; Roman, M. J.; Decker, E. A.; Goddard, J. M. Synthesis of Iminodiacetate Functionalized Polypropylene Films and Their Efficacy as Antioxidant Active-Packaging Materials. *J. Agric. Food Chem.* **2016**, *64* (22), 4606−17.

(12) Tian, F.; Decker, E. A.; Goddard, J. M. Control of Lipid Oxidation by Nonmigratory Active Packaging Films Prepared by Photoinitiated Graft Polymerization. *J. Agric. Food Chem.* **2012**, *60* (31), 7710−8.

(13) Hazer, B.; Ashby, R. D. Synthesis of a Novel Tannic Acid-Functionalized Polypropylene as Antioxidant Active-Packaging Materials. *Food Chem.* **2021**, *344*, 128644.

(14) Doshna, N. A.; Herskovitz, J. E.; Redfearn, H. N.; Goddard, J. M. Antimicrobial Active Packaging Prepared by Reactive Extrusion of E-Poly L-Lysine with Polypropylene. *ACS Food Science & Technology.* **2022**, *2*, 391.

(15) Werner, B. G.; Koontz, J. L.; Goddard, J. M. Hurdles to Commercial Translation of Next Generation Active Food Packaging Technologies. *Current Opinion in Food Science.* **2017**, *16*, 40−8.

(16) Moad, G. The Synthesis of Polyolefin Graft Copolymers by Reactive Extrusion. *Prog. Polym. Sci.* **1999**, *24* (1), 81−142.

(17) Badrossamay, M. R.; Sun, G. Durable and Rechargeable Biocidal Polypropylene Polymers and Fibers Prepared by Using Reactive Extrusion. *Journal of Biomedical Materials Research Part B: Applied Biomaterials.* **2009**, *89B* (1), 93−101.

(18) Hassouna, F.; Raquez, J.-M.; Addiego, F.; Dubois, P.; Toniazzo, V.; Ruch, D. New Approach on the Development of Plasticized Polylactide (Pla), Grafting of Poly(Ethylene Glycol) (Peg) Via Reactive Extrusion. *Eur. Polym. J.* **2011**, *47* (11), 2134−44.

(19) Wang, D.; Xu, W.; Sun, G.; Chiou, B-s. Radical Graft Polymerization of an Allyl Monomer onto Hydrophilic Polymers and Their Antibacterial Nanofibrous Membranes. *ACS Appl. Mater. Interfaces.* **2011**, *3* (8), 2838−44.

(20) Herskovitz, J. E.; Goddard, J. M. Antioxidant Functionalization of Biomaterials Via Reactive Extrusion. *J. Appl. Polym. Sci.* **2021**, *138* (25), 50591.

(21) Kay, I. P.; Herskovitz, J. E.; Goddard, J. M. Interfacial Behavior of a Polylactic Acid Active Packaging Film Dictates Its Performance in Complex Food Matrices. *Food Packaging and Shelf Life.* **2022**, *32*, 100832.

(22) Sharifi-Rad, J.; Rayess, Y. E.; Rizk, A. A.; Sadaka, C.; Zgheib, R.; Zam, W.; et al. Turmeric and Its Major Compound Curcumin on Health: Bioactive Effects and Safety Profiles for Food, Pharmaceutical, Biotechnological and Medicinal Applications. *Frontiers in Pharmacology.* **2020**, *11*, 01021.

(23) Zorofchian Moghadamtousi, S.; Abdul Kadir, H.; Hassandarvish, P.; Tajik, H.; Abubakar, S.; Zandi, K. A Review on Antibacterial, Antiviral, and Antifungal Activity of Curcumin. *BioMed. Research International.* **2014**, *2014*, 186864.

(24) Mary, C. P. V.; Vijayakumar, S.; Shankar, R. Metal Chelating Ability and Antioxidant Properties of Curcumin-Metal Complexes − a Dft Approach. *J. Mol. Graphics Modell.* **2018**, *79*, 1−14.

(25) Roy, S.; Priyadarshi, R.; Ezati, P.; Rhim, J.-W. Curcumin and Its Uses in Active and Smart Food Packaging Applications - a Comprehensive Review. *Food Chem.* **2022**, *375*, 131885.

(26) Zhai, X.; Wang, X.; Zhang, J.; Yang, Z.; Sun, Y.; Li, Z.; et al. Extruded Low Density Polyethylene-Curcumin Film: A Hydrophobic Ammonia Sensor for Intelligent Food Packaging. *Food Packaging and Shelf Life.* **2020**, *26*, 100595.

(27) Roy, S.; Rhim, J.-W. Preparation of Bioactive Functional Poly(Lactic Acid)/Curcumin Composite Film for Food Packaging Application. *Int. J. Biol. Macromol.* **2020**, *162*, 1780−9.

(28) Roy, S.; Rhim, J.-W. Curcumin Incorporated Poly(Butylene Adipate-Co-Terephthalate) Film with Improved Water Vapor Barrier and Antioxidant Properties. *Materials* **2020**, *13* (19), 4369.

(29) Cvek, M.; Paul, U. C.; Zia, J.; Mancini, G.; Sedlarik, V.; Athanassiou, A. Biodegradable Films of Pla/Ppc and Curcumin as Packaging Materials and Smart Indicators of Food Spoilage. *ACS Appl. Mater. Interfaces.* **2022**, *14* (12), 14654−67.

(30) Yildiz, E.; Sumnu, G.; Kahyaoglu, L. N. Monitoring Freshness of Chicken Breast by Using Natural Halochromic Curcumin Loaded Chitosan/Peo Nanofibers as an Intelligent Package. *Int. J. Biol. Macromol.* **2021**, *170*, 437−46.

(31) Curcio, M.; Puoci, F.; Iemma, F.; Parisi, O. I.; Cirillo, G.; Spizzirri, U. G.; et al. Covalent Insertion of Antioxidant Molecules on Chitosan by a Free Radical Grafting Procedure. *J. Agric. Food Chem.* **2009**, *57* (13), 5933−8.

(32) Cirillo, G.; Hampel, S.; Klingeler, R.; Puoci, F.; Iemma, F.; Curcio, M.; et al. Antioxidant Multi-Walled Carbon Nanotubes by Free Radical Grafting of Gallic Acid: New Materials for Biomedical Applications. *J. Pharm. Pharmacol.* **2011**, *63* (2), 179−88.

(33) Spizzirri, U. G.; Altimari, I.; Puoci, F.; Parisi, O. I.; Iemma, F.; Picci, N. Innovative Antioxidant Thermo-Responsive Hydrogels by Radical Grafting of Catechin on Inulin Chain. *Carbohydr. Polym.* **2011**, *84* (1), 517−23.

(34) Cho, Y.-S.; Kim, S.-K.; Ahn, C.-B.; Je, J.-Y. Preparation, Characterization, and Antioxidant Properties of Gallic Acid-Grafted-Chitosans. *Carbohydr. Polym.* **2011**, *83* (4), 1617−22.

(35) Uyama, H.; Maruichi, N.; Tonami, H.; Kobayashi, S. Peroxidase-Catalyzed Oxidative Polymerization of Bisphenols. *Biomacromolecules.* **2002**, *3* (1), 187−93.

(36) Kobayashi, S.; Higashimura, H. Oxidative Polymerization of Phenols Revisited. *Prog. Polym. Sci.* **2003**, *28* (6), 1015−48.

(37) Priyadarsini, K. I.; Maity, D. K.; Naik, G. H.; Kumar, M. S.; Unnikrishnan, M. K.; Satav, J. G.; et al. Role of Phenolic O-H and Methylene Hydrogen on the Free Radical Reactions and Antioxidant Activity of Curcumin. *Free Radical Biol. Med.* **2003**, *35* (5), 475−84.

(38) Redfearn, H. N.; Goddard, J. M. Antioxidant and Dissociation Behavior of Polypropylene-Graft-Maleic Anhydride. *J. Appl. Polym. Sci.* **2022**, *139* (32), No. e52764.

(39) FDA. Guidance for Industry: Preparation of Premarket Submissions for Food Contact Substances (Chemistry Recommen-

https://doi.org/10.1021/acsami.3c06589
ACS Appl. Mater. Interfaces 2023, 15, 29511−29524

dations), 2018. Available from: https://www.fda.gov/regulatory-information/search-fda-guidance-documents/guidance-industry-preparation-premarket-submissions-food-contact-substances-chemistry#ai.
(40) EU. Commission Regulation (Eu) No 10/20/2011 on Plastic Materials and Articles Intended to Come into Contact with Food. *Official Journal of the European Union* **2011**, *045*, 42−130.
(41) Roy, S.; Rhim, J.-W. Carboxymethyl Cellulose-Based Antioxidant and Antimicrobial Active Packaging Film Incorporated with Curcumin and Zinc Oxide. *Int. J. Biol. Macromol.* **2020**, *148*, 666−76.
(42) Horwitz, W *Association of Official Analytical Chemists. Official Methods of Analysis of the Association of Official Analytical Chemists*; The Association: Washington, DC, 1970; p 5.
(43) Association JS. Antimicrobial Products: Test for Antimicrobial Activity and Efficacy. Japanese Industrial Standard, 2000; JIS Z 2801, 2000.
(44) Shi, D.; Yang, J.; Yao, Z.; Wang, Y.; Huang, H.; Jing, W.; et al. Functionalization of Isotactic Polypropylene with Maleic Anhydride by Reactive Extrusion: Mechanism of Melt Grafting. *Polymer.* **2001**, *42* (13), 5549−57.
(45) Farahanchi, A.; Malloy, R.; Sobkowicz, M. J. Effects of Ultrahigh Speed Twin Screw Extrusion on the Thermal and Mechanical Degradation of Polystyrene. *Polymer Engineering & Science.* **2016**, *56* (7), 743−51.
(46) Esatbeyoglu, T.; Ulbrich, K.; Rehberg, C.; Rohn, S.; Rimbach, G. Thermal Stability, Antioxidant, and Anti-Inflammatory Activity of Curcumin and Its Degradation Product 4-Vinyl Guaiacol. *Food Funct.* **2015**, *6* (3), 887−93.
(47) Azizi, H.; Ghasemi, I. Reactive Extrusion of Polypropylene: Production of Controlled-Rheology Polypropylene (Crpp) by Peroxide-Promoted Degradation. *Polym. Test.* **2004**, *23* (2), 137−43.
(48) Nakason, C.; Saiwari, S.; Kaesaman, A. Rheological Properties of Maleated Natural Rubber/Polypropylene Blends with Phenolic Modified Polypropylene and Polypropylene-G-Maleic Anhydride Compatibilizers. *Polym. Test.* **2006**, *25* (3), 413−23.
(49) de Campos, S. S.; de Oliveira, A.; Moreira, T. F. M.; da Silva, T. B. V.; da Silva, M. V.; Pinto, J. A.; et al. Tpcs/Pbat Blown Extruded Films Added with Curcumin as a Technological Approach for Active Packaging Materials. *Food Packaging and Shelf Life.* **2019**, *22*, 100424.
(50) Tsekova, P. B.; Spasova, M. G.; Manolova, N. E.; Markova, N. D.; Rashkov, I. B. Electrospun Curcumin-Loaded Cellulose Acetate/Polyvinylpyrrolidone Fibrous Materials with Complex Architecture and Antibacterial Activity. *Materials Science and Engineering: C* **2017**, *73*, 206−14.
(51) Krump, H.; Luyt, A. S.; Molefi, J. A. Changes in Free Surface Energy as an Indicator of Polymer Blend Miscibility. *Mater. Lett.* **2005**, *59* (4), 517−9.
(52) Zografi, G.; Johnson, B. A. Effects of Surface Roughness on Advancing and Receding Contact Angles. *Int. J. Pharm.* **1984**, *22* (2), 159−76.
(53) Duvall, J.; Sellitti, C.; Myers, C.; Hiltner, A.; Baer, E. Interfacial Effects Produced by Crystallization of Polypropylene with Polypropylene-G-Maleic Anhydride Compatibilitzers. *J. Appl. Polym. Sci.* **1994**, *52* (2), 207−16.
(54) Seo, Y.; Kim, J.; Kim, K. U.; Kim, Y. C. Study of the Crystallization Behaviors of Polypropylene and Maleic Anhydride Grafted Polypropylene. *Polymer.* **2000**, *41* (7), 2639−46.
(55) Priyadarsini, K. I. The Chemistry of Curcumin: From Extraction to Therapeutic Agent. *Molecules.* **2014**, *19* (12), 20091−112.
(56) Guzman-Puyol, S.; Hierrezuelo, J.; Benítez, J. J.; Tedeschi, G.; Porras-Vázquez, J. M.; Heredia, A.; et al. Transparent, Uv-Blocking, and High Barrier Cellulose-Based Bioplastics with Naringin as Active Food Packaging Materials. *Int. J. Biol. Macromol.* **2022**, *209*, 1985−94.
(57) Choe, E.; Min, D. B. Chemistry and Reactions of Reactive Oxygen Species in Foods. *J. Food Sci.* **2005**, *70* (9), R142−R59.
(58) Floegel, A.; Kim, D.-O.; Chung, S.-J.; Koo, S. I.; Chun, O. K. Comparison of Abts/Dpph Assays to Measure Antioxidant Capacity in Popular Antioxidant-Rich Us Foods. *Journal of Food Composition and Analysis.* **2011**, *24* (7), 1043−8.
(59) Romani, V. P.; Martins, V. G.; Goddard, J. M. Radical Scavenging Polyethylene Films as Antioxidant Active Packaging Materials. *Food Control.* **2020**, *109*, 106946.
(60) Litwinienko, G.; Ingold, K. U. Abnormal Solvent Effects on Hydrogen Atom Abstraction. 2. Resolution of the Curcumin Antioxidant Controversy. The Role of Sequential Proton Loss Electron Transfer. *J. Org. Chem.* **2004**, *69* (18), 5888−96.
(61) Shaikh, S. A. M.; Singh, B. G.; Barik, A.; Balaji, N. V.; Subbaraju, G. V.; Naik, D. B.; et al. Unravelling the Effect of B-Diketo Group Modification on the Antioxidant Mechanism of Curcumin Derivatives: A Combined Experimental and Dft Approach. *J. Mol. Struct.* **2019**, *1193*, 166−76.
(62) Zebib, B.; Mouloungui, Z.; Noirot, V. Stabilization of Curcumin by Complexation with Divalent Cations in Glycerol/Water System. *Bioinorg Chem. Appl.* **2010**, *2010*, 292760.
(63) Ozgen, M.; Reese, R. N.; Tulio, A. Z.; Scheerens, J. C.; Miller, A. R. Modified 2,2-Azino-Bis-3-Ethylbenzothiazoline-6-Sulfonic Acid (Abts) Method to Measure Antioxidant Capacity of Selected Small Fruits and Comparison to Ferric Reducing Antioxidant Power (Frap) and 2,2‘-Diphenyl-1-Picrylhydrazyl (Dpph) Methods. *J. Agric. Food Chem.* **2006**, *54* (4), 1151−7.
(64) Zwirzitz, B.; Wetzels, S. U.; Dixon, E. D.; Stessl, B.; Zaiser, A.; Rabanser, I.; et al. The Sources and Transmission Routes of Microbial Populations Throughout a Meat Processing Facility. *NPJ Biofilms Microbiomes* **2020**, *6* (1), 26.
(65) Gunes, H.; Gulen, D.; Mutlu, R.; Gumus, A.; Tas, T.; Topkaya, A. E. Antibacterial Effects of Curcumin:An in Vitro Minimum Inhibitory Concentration Study. *Toxicology and Industrial Health.* **2016**, *32* (2), 246−50.
(66) Almeida, H. H. S.; Barros, L.; Barreira, J. C. M.; Calhelha, R. C.; Heleno, S. A.; Sayer, C.; et al. Bioactive Evaluation and Application of Different Formulations of the Natural Colorant Curcumin (E100) in a Hydrophilic Matrix (Yogurt). *Food Chem.* **2018**, *261*, 224−32.
(67) Yadav, S.; Singh, A. K.; Agrahari, A. K.; Sharma, K.; Singh, A. S.; Gupta, M. K.; Tiwari, V. K.; Prakash, P.; et al. Making of Water Soluble Curcumin to Potentiate Conventional Antimicrobials by Inducing Apoptosis-Like Phenomena among Drug-Resistant Bacteria. *Sci. Rep.* **2020**, *10* (1), 14204.

https://doi.org/10.1021/acsami.3c06589
ACS Appl. Mater. Interfaces 2023, 15, 29511−29524